Activation and labelling of the purified skeletal muscle ryanodine receptor by an oxidized ATP analogue

Martin HOHENEGGER,*‡ Annegret HERRMANN-FRANK,† Michael RICHTER† and Frank LEHMANN-HORN†

*Institute of Pharmacology, University of Vienna, Währingerstrasse 13a, A-1090 Vienna, Austria,
and †Department of Applied Physiology, University of Ulm, D-89069 Ulm, Germany

We have tested the periodate-oxidized ATP analogue 2′,3′-dialdehyde adenosine triphosphate (oATP) as a ligand for the skeletal muscle ryanodine receptor/Ca^{2+}-release channel. Ca^{2+} efflux from passively loaded heavy sarcoplasmic reticulum vesicles of skeletal muscle is biphasic. oATP stimulates the initial phase of Ca^{2+} release in a concentration-dependent manner (EC_{50} 160 μM), and the efflux proceeds with a half-time in the range 100–200 ms. This oATP-modulated initial rapid Ca^{2+} release was specifically inhibited by millimolar concentrations of Mg^{2+} and micromolar concentrations of Ruthenium Red, indicating that the effect of oATP was mediated via the ryanodine receptor. The purified Ca^{2+}-release channel was incorporated into planar lipid bilayers, and single-channel recordings were carried out to verify a direct interaction of oATP with the ryanodine receptor. Addition of oATP to the cytoplasmic side activated the channel with an EC_{50} of 76 μM, which is roughly 30-fold higher than the apparent affinity of ATP. The oATP-induced increase in the open probability of the ryanodine receptor displays a steep concentration–response curve with a Hill coefficient of ~ 2, which suggests a co-operativity of the ATP binding sites in the tetrameric protein. oATP binds to the ryanodine receptor in a quasi-irreversible manner via Schiff base formation between the aldehyde groups of oATP and amino groups in the nucleotide binding pocket. This allows for the covalent specific incorporation of [α-^{32}P]oATP by borhydride reduction. A typical adenine nucleotide binding site cannot be identified in the primary sequence of the ryanodine receptor. Our results demonstrate that oATP can be used to probe the structure and function of the nucleotide binding pocket of the ryanodine receptor and presumably of other ATP-regulated ion channels.

INTRODUCTION

Skeletal muscle contraction and relaxation is regulated by the myoplasmic free Ca^{2+} concentration [1,2]. Ca^{2+} is stored in the sarcoplasmic reticulum (SR), where it is pumped by a Ca^{2+}-transporting ATPase [2]. Following muscle excitation, contraction is initiated by rapid Ca^{2+} release from the internal Ca^{2+} store. Using the plant alkaloid ryanodine, the high-molecular-mass ryanodine receptor protein was purified and identified as the Ca^{2+}-release channel of the terminal cisternae of the SR [3–5]. The pharmacology of the ryanodine receptor includes inhibition by cytoplasmic Mg^{2+}, Ruthenium Red and calmodulin, while activation is achieved by micromolar concentrations of cytoplasmic Ca^{2+} and various exogenous ligands such as the methylxanthine caffeine and the anthracycline doxorubicin (for review see [6]). Adenine nucleotides are also involved in the modulation of ryanodine receptor/Ca^{2+}-release channel activity. ATP acts as the phosphate donor for regulatory phosphorylation by various protein kinases [7–10]. In addition, adenine nucleotides induce Ca^{2+} release from isolated SR vesicles [11,12]. This effect is thought to result from direct interaction with the ryanodine receptor, since a stimulation of channel gating can be observed in single-channel recordings following insertion of the purified receptor into planar lipid bilayers [13,14]. However, the deduced amino acid sequence of the ryanodine receptor does not predict a typical ATP binding domain [15,16].

We have therefore tested the 2′,3′-dialdehyde ATP analogue oATP for its ability to activate the ryanodine receptor and to label the nucleotide binding site of the protein. Previous experiments have verified that oATP is a useful tool with which to label the catalytic adenine nucleotide binding site of the Ca^{2+}-ATPase from the SR [17]. Due to the presence of the aldehyde groups, oATP can form stable Schiff bases with ϵ-amino groups of lysine residues in the nucleotide binding cleft and can be covalently incorporated into the enzyme.

In the present paper we show that oATP is a potent stimulator of Ca^{2+} release, an effect exerted via direct interaction with the ryanodine receptor. In addition, oATP can be covalently incorporated into the adenine nucleotide binding site of the ryanodine receptor.

MATERIALS AND METHODS

Materials

ATP and ADP were purchased from Boehringer (Mannheim, Germany); Rotiszint scintillator from Roth (Karlsruhe, Germany); Ruthenium Red and low-molecular-mass protein standards from Sigma Chemical Co. (St. Louis, MO, U.S.A.); high-molecular-mass standard kit from Pharmacia (Freiburg, Germany); lipids from Avanti Polar Lipids (Alabaster, AL, U.S.A.); ryanodine from Calbiochem (San Diego, CA, U.S.A.); [α-^{32}P]ATP from NEN (Boston, MA, U.S.A.); and $^{45}CaCl_2$ from Amersham Buchler (Braunschweig, Germany). All other reagents were of analytical grade.

Synthesis of oATP

Sodium periodate-oxidized ATP, oATP, was synthesized according to the method of Easterbrook-Smith et al. [18]. Purity

Abbreviations used: (H)SR, (heavy) sarcoplasmic reticulum; oATP, 2′,3′-dialdehyde adenosine triphosphate; P_o, open probability.

‡ To whom correspondence should be addressed.

and concentration were controlled by HPLC, TLC and spectrometry as described previously [17]. ATP or [α-^{32}P]ATP was used as the starting material.

Membrane preparation and protein purification

Heavy SR (HSR) from rabbit hind leg white muscle was prepared according to Wyskovsky et al. [19]. Purification of the ryanodine receptor from skeletal HSR was achieved using a combination of sucrose density centrifugation and chromatography with a heparin–agarose column [20]. For single-channel recordings, HSR vesicles were isolated from rabbit back muscles. The ryanodine receptor was purified by solubilization of HSR vesicles in CHAPS, followed by sucrose density gradient centrifugation in the presence of CHAPS and exogenous phospholipids as previously described [9]. The two preparations were equivalent with respect to [^{3}H]ryanodine binding. Ryanodine receptors purified from both types of HSR preparations were used for oATP labelling experiments and gave identical results.

Ca^{2+} release measurements

HSR vesicles (10 mg/ml) were passively loaded in a medium containing 50 mM Mops (pH 7.0), 80 mM KCl, 5 mM NaN_3 and 15 mM $^{45}CaCl_2$ (specific radioactivity 100–500 c.p.m./nmol) at 4 °C. After 24–48 h release experiments were started, using the Bio-Logic rapid-filtration system [21]. The steady-state accumulation amounted to 130–150 nmol of Ca^{2+}/mg of HSR, and the variation between the individual preparations was in the range 10–20 %.

The passively loaded vesicles were diluted 200-fold into a volume of 2 ml in the same medium supplemented with 1 mM EGTA and 5 mM $MgCl_2$, but lacking $CaCl_2$. Subsequently, 1 ml of the diluted protein was applied on to the filter (Schleicher & Schuell filters; ME 26; 0.6 μm) of the rapid filtration apparatus and rinsed with release medium containing 50 mM Mops (pH 7.0), 80 mM KCl, 5 mM NaN_3, 0.5 mM $CaCl_2$ and 0.5 mM EGTA. The concentrations of added adenine nucleotides are indicated in the Figure legends. For inhibition experiments, the release medium was supplemented with 5 mM $MgCl_2$ or 20 μM Ruthenium Red. For incubation times longer than 10 s, a manual filtration device (Millipore) was used. The dilution of the loaded vesicles in the manual filtration assay was carried out directly into the release medium. Ca^{2+} release was stopped with 20 μM Ruthenium Red and 5 mM $MgCl_2$ at the time points given in Figure 1. After filtration of the vesicles, the filters (Schleicher & Schuell; BA 85; 0.45 μm) were rinsed twice with 3 ml of 50 mM Mops (pH 7.0), 5 mM NaN_3, 80 mM KCl, 5 mM $MgCl_2$ and 20 μM Ruthenium Red. The radioactivity trapped on the filters was determined by liquid scintillation counting. Blanks without protein were subtracted. Data points represent means of duplicates. All release experiments were performed at 22 °C.

Measurements in planar lipid bilayers

The purified ryanodine receptor was incorporated into planar lipid bilayers formed from a mixture of phosphatidylethanolamine/phosphatidylserine/L-α-diphytanoylphosphatidylcholine in the proportions 5:4:1 (20 mg/ml phospholipid in decane). Using K^+ as a charge carrier, reconstitution was carried out in symmetrical buffer solutions containing 250 mM KCl, 150 μM Ca^{2+}, 100 μM EGTA and 20 mM Pipes (pH 7.2). Small aliquots of the solubilized ryanodine receptor (< 1 μg of protein) were added to the *cis* side of the bilayer membrane, defined as the cytoplasmic side of the channel. Successful incorporation of channels was detected as a step-wise increase in current. Electrical signals were filtered at 1 kHz through an 8-pole-pass bessel filter and digitized at 3 kHz. Acquired data were stored online and analysed on an IBM-compatible AT-computer using Axon Instruments hardware and software. Open probability (P_o) values were calculated from representative data segments of 20 s duration selected from total recording times of about 3 min for any condition tested. The indicated holding potentials were applied with reference to the *trans* chamber. Experiments were carried out at 22 °C.

Affinity labelling with oATP

The purified ryanodine receptor (0.5–0.7 μg) was incubated in 20 μl of 20 mM Tris/HCl (pH 7.6), 30 μM $CaCl_2$, 5 mM $MgCl_2$ and [α-^{32}P]oATP (specific radioactivity 12–60 c.p.m./nmol) at the concentrations indicated in the legend to Figure 5 in the absence and presence of competing adenine nucleotides. The incubation was carried out at 20 °C in the dark. At the time points indicated in the legend to Figure 5, reduction was initiated by the addition of 80 mM $NaCNBH_3$ (for 1 min at 25 °C) followed by the addition of 10 mM $NaBH_4$ (for 1 h on ice). In order to remove the free radioactive nucleotide, the samples containing 50 μM [α-^{32}P]oATP were subsequently dialysed against 20 mM Tris/HCl (pH 7.0), 30 μM $CaCl_2$, 5 mM $MgCl_2$ and 5 mM NaN_3 at 4 °C. Alternatively, samples containing 10 μM [α-^{32}P]oATP were directly diluted in 2 × Laemmli sample buffer, to which mercaptoethanol (1 % final) had been added. The samples were heated at 95 °C for 2 min and subjected to electrophoresis [22]. The ryanodine receptor was resolved on discontinuous SDS/polyacrylamide gels (5 % stacking gel; 7 % separating gel). The exposure time for autoradiography varied from 12 to 72 h, using Kodak-XS films. Molecular mass standards were thyroglobulin (330 kDa), ferritin (220 kDa), albumin (67 kDa), catalase (60 kDa) and lactate dehydrogenase (36 kDa).

Miscellaneous procedures

Protein concentration was measured according to the method of Lowry et al. [23] or Kaplan and Pedersen [24], using BSA as standard. Free Ca^{2+} concentrations were calculated by a computer program using binding constants published by Fabiato [25]. Data were fitted by non-linear least-squares regression to appropriate equations (mono- and bi-exponential decay; Hill equation) using the Gauss–Newton or Marquardt–Levenberg algorithm.

RESULTS

oATP-induced $^{45}Ca^{2+}$ release

The periodate-oxidized ATP analogue oATP was investigated for its ability to induce Ca^{2+} release from passively loaded skeletal muscle HSR. Passive loading was chosen because, under these conditions, exogenous nucleotides are not carried over from the loading procedure and thus cannot interfere with the subsequent release measurements with oATP. In the absence of Mg^{2+}, addition of oATP led to a rapid release of Ca^{2+}, which was similar in extent to that produced by equimolar concentrations of AMP. Within 10 s, 60 % of the loaded Ca^{2+} was released by both nucleotides (Figure 1a). In order to characterize the kinetics of this initial fast release phase, a rapid filtration device was used. The time-resolved oATP-induced Ca^{2+} release is shown in Figure 1(b). In the presence of 500 μM oATP, Ca^{2+} release followed a biphasic time course as described previously for AMP, adenosine 5′-[$\beta\gamma$-methylene]triphosphate and ATP [19,26]. The initial fast

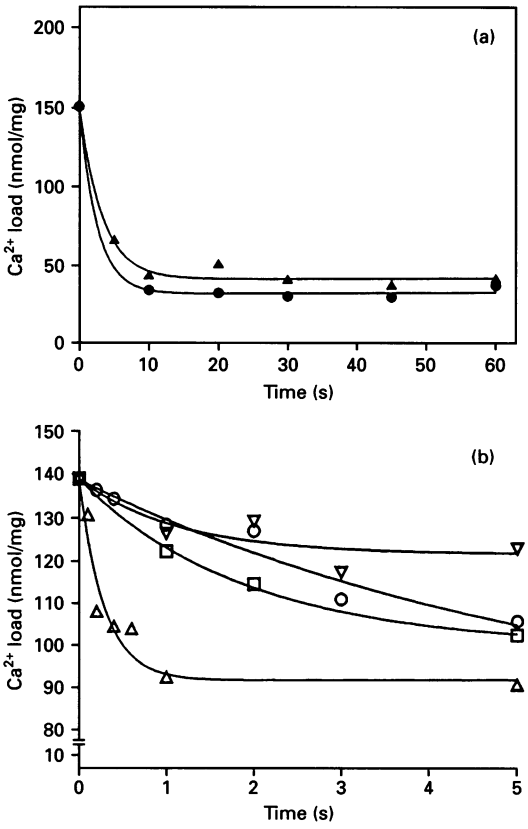

Figure 1 oATP-induced Ca^{2+} release from passively loaded SR vesicles

(**a**) Comparison of AMP- and oATP-induced Ca^{2+} release. Passively loaded SR vesicles (10 mg/ml) were diluted into a medium containing 50 mM Mops (pH 7.0), 80 mM KCl, 5 mM NaN_3, 0.5 mM $CaCl_2$, 0.5 mM EGTA and 1 mM AMP (●) or 1 mM oATP (▲) to give a protein concentration of 0.05 mg/ml. At the time points indicated, the reaction (1 ml) was quenched by the addition of $MgCl_2$ and Ruthenium Red to give final concentrations of 5 mM and 20 μM respectively. The samples were filtered and the radioactivity remaining on the filters was determined by liquid scintillation counting. (**b**) Rapid activation and inhibition of oATP-induced Ca^{2+} release. Passively loaded SR vesicles (10 mg/ml) were diluted 200-fold in 50 mM Mops (pH 7.0), 80 mM KCl, 5 mM NaN_3, 5 mM $MgCl_2$ and 2 mM EGTA. Subsequently, aliquots (1 ml) were applied on to the filter of the rapid filtration apparatus. The filters were rinsed with the release medium containing 50 mM Mops (pH 7.0), 80 mM KCl, 5 mM NaN_3, 0.5 mM $CaCl_2$ and 0.5 mM EGTA for the indicated times. Then 10 μM oATP (□), 500 μM oATP (△), 500 μM oATP plus 5 mM $MgCl_2$ (○) or 500 μM oATP plus 20 μM Ruthenium Red (▽) were added to the release medium. Data points represent the means of duplicate determinations in a single experiment which was repeated three times with different preparations.

Table 1 Comparison of the amplitudes (*A*) and rates (*k*) of the first and second Ca^{2+} release phases from passively loaded SR

The first and second Ca^{2+} release phases were calculated from experiments performed under conditions given in the legend to Figure 1(b). The experimental data points were fitted according to one or two exponential functions by non-linear least-squares regression. Mean values ± S.E.M. of three experiments are presented. RR, Ruthenium Red.

	A_1 (nmol/mg)	$k_{(1)}$ (s^{-1})	A_2 (nmol/mg)	$k_{(2)}$ (s^{-1})
10 μM oATP	–	–	62.6 ± 38.3	0.16 ± 0.12
500 μM oATP	43.5 ± 2.8	4.4 ± 1.0	48.5 ± 3.5	0.1 ± 0.05
500 μM oATP + 5 mM Mg^{2+}	–	–	97.3 ± 33.8	0.6 ± 0.3
500 μM oATP + 20 μM RR	–	–	42.2 ± 7.0	0.55 ± 0.21

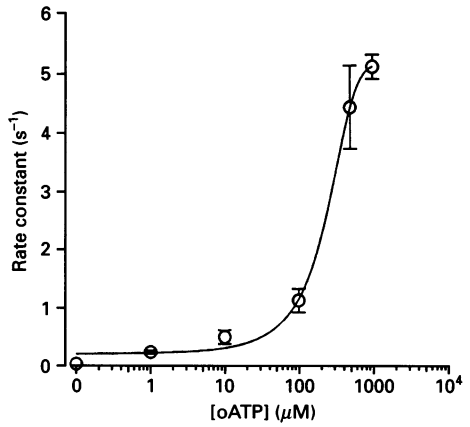

Figure 2 Concentration–response curve for oATP-induced Ca^{2+} release

The rate constants of the first Ca^{2+}-release phase at the oATP concentrations indicated were determined as described in the legend to Table 1. The mean rates (n = 3) were plotted against the oATP concentration. Error bars indicate S.D.

phase of Ca^{2+} release proceeds with a half-time of about 100–200 ms (Table 1). This oATP-induced Ca^{2+} release was completely inhibited by millimolar concentrations of Mg^{2+} and micromolar concentrations of Ruthenium Red, suggesting that the effect of oATP depends on calcium movement through the ryanodine receptor/Ca^{2+}-release channel. The second phase of Ca^{2+} release displays a half-time in the range of 1–8 s (Table 1). We were not able to detect any significant change in parameters within this phase that would indicate regulation by oATP.

A steep concentration–response curve was observed for the oATP-induced stimulation of Ca^{2+} release (Figure 2). When the data were fitted to the Hill equation using a non-linear least-squares algorithm, an EC_{50} of 160–200 μM and a slope of 1.7 were estimated. However, the estimation of both parameters, the apparent affinity as well as the Hill coefficient, were affected by non-equilibrium conditions. Over the time-scale of < 1s, the association rate for oATP at low concentrations is too slow to allow for equilibrium binding to the Ca^{2+}-release channel (see Figure 5c). Hence the calculated EC_{50} underestimates the true affinity. This interpretation is substantiated by the higher affinity of oATP for the ryanodine receptor, which was observed in the single-channel recordings described below. Similarly, due to the non-equilibrium conditions, the calculated Hill coefficient cannot serve as a reliable estimate for the true co-operativity.

Single-channel recording of the purified ryanodine receptor

In order to prove the direct interaction of oATP with the ryanodine receptor, the purified receptor was incorporated into planar lipid bilayers to study the gating behaviour of the isolated channel. In the presence of submicromolar Ca^{2+} concentrations, addition of oATP to the *cis* side of the bilayer chamber activated the channel in a concentration-dependent manner (Figure 3a). As expected from the activation with ATP, the Ca^{2+}-release channel did not show a change in conductance following oATP treatment (results not shown). An increase in the P_o was observed with oATP concentrations of $\geq$ 30 μM (Figure 3b), a concentration range which also triggered $^{45}Ca^{2+}$-release. The maximum stimulatory effect was reached at about 300–400 μM oATP.

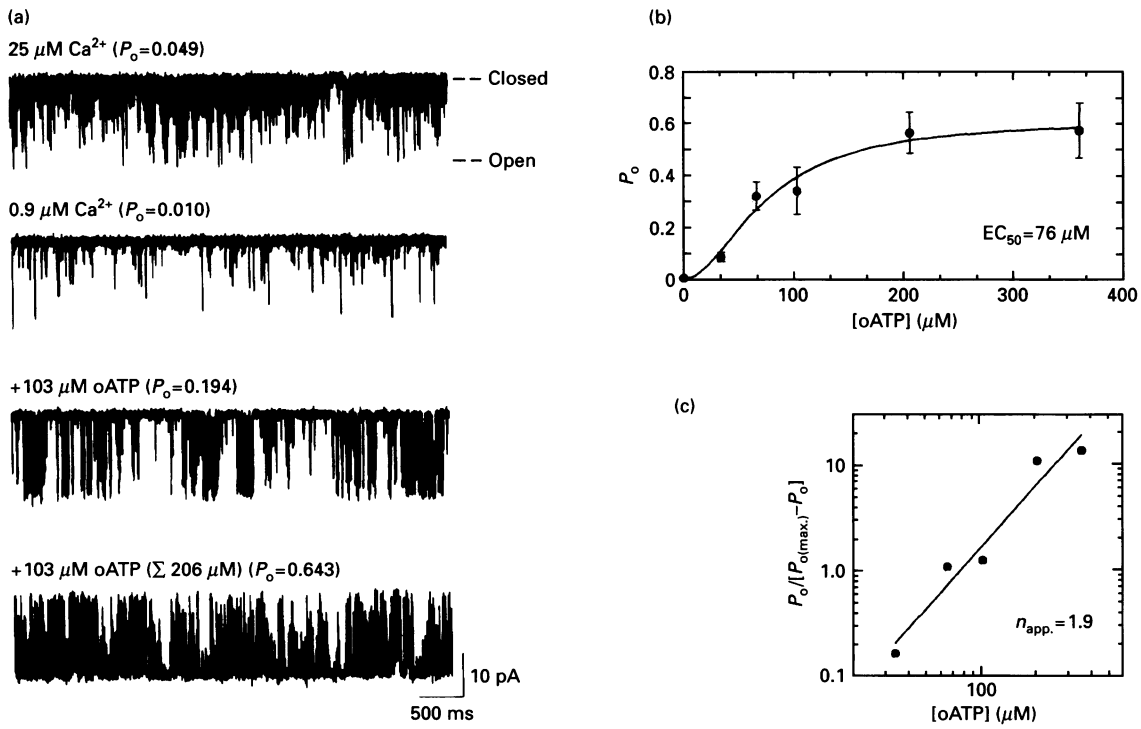

Figure 3 oATP-induced activation of the isolated ryanodine receptor/Ca^{2+}-release channel

(**a**) Single-channel K^+ currents of the purified ryanodine receptor were measured in the presence of the indicated free Ca^{2+} concentrations and of increasing concentrations of oATP, which were successively added to the *cis* side of the channel. P_o values were calculated from data segments of 20 s duration. The holding potential was −30 mV. Voltages were applied with reference to the *trans* chamber. (**b**) Increasing concentrations of oATP were applied to the *cis* chamber. Data were taken from representative single-channel recordings ($n = 5$) in the presence of 0.9 μM *cis* Ca^{2+}. Data were fitted according to the Hill equation. Error bars represent S.D. (**c**) Linearized transformation (Hill plot) of (**b**). The means of the P_o values in (**b**) were used for calculation.

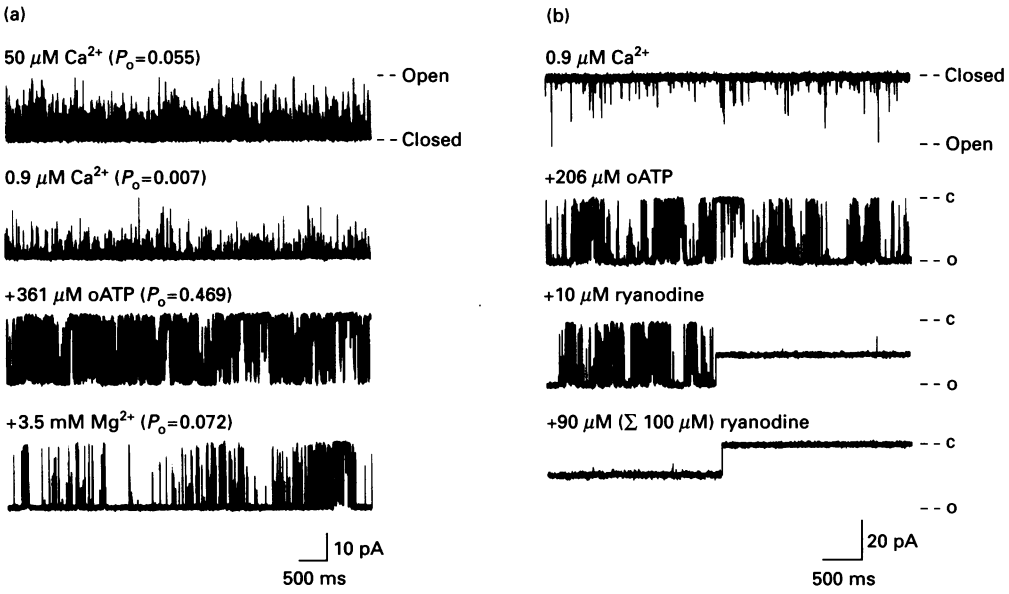

Figure 4 Modulation of the oATP-activated Ca^{2+}-release channel by Mg^{2+} (a) and ryanodine (b)

(**a**) All effectors were successively added to the *cis* side of the channel as outlined in the legend to Figure 3 (**a**). The holding potential was 49 mV. (**b**) Modulation and inhibition of the oATP-activated channel by 10 and 100 μM ryanodine respectively. The holding potential was −62 mV.

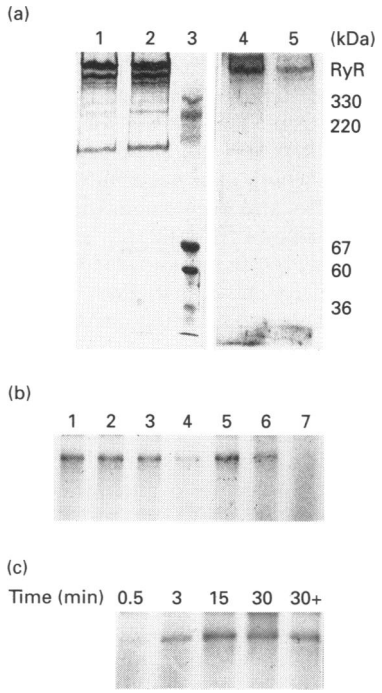

Figure 5 [α^{32}P]oATP labelling of the ryanodine receptor from skeletal muscle

(**a**) The purified ryanodine receptor (RyR; 0.7 μg) was incubated with 50 μM [[α-^{32}P]oATP (specific radioactivity 12 c.p.m./nmol) in the absence (lanes 1 and 4) and presence (lanes 2 and 5) of 1 mM ADP. After 30 min at 22 °C, the samples were reduced as described in the Materials and methods section and subsequently applied to an SDS/7% polyacrylamide gel. Lane 3 contains molecular mass standards. The proteins were visualized by staining with Coomassie Blue (lanes 1–3); autoradiography was carried out on the dried gel (lanes 4 and 5) for 48 h at room temperature using an intensifying screen. (**b**) The purified ryanodine receptor (0.7 μg) was incubated with 10 μM [α-^{32}P]oATP (specific radioactivity 60 c.p.m./nmol) at 22 °C in the absence (lane 1) and presence of 0.1 mM, 1 mM or 10 mM ATP (lanes 2–4 respectively) or oATP (lanes 5–7 respectively). After 10 min, the samples were reduced as described in the Materials and methods section. Only the high-molecular-mass region of the autoradiogram (48 h exposure) is shown. (**c**) The incubation was carried out with 10 μM [α-^{32}P]oATP (specific radioactivity 60 c.p.m./nmol) at 22 °C. At the time points indicated (lanes 1–4), aliquots containing 0.7 μg of purified ryanodine receptor were withdrawn and reduction was carried out as outlined in the Materials and methods section. Lane 30+, after a 15 min preincubation of 0.7 μg of purified ryanodine receptor with 10 μM [α-^{32}P]oATP, 10 mM ATP was added to the sample and the incubation was continued for an additional 15 min and reduced thereafter. Only the high-molecular-mass region of the autoradiogram (72 h exposure) is shown.

When the P_o was plotted versus the applied oATP concentration, an EC_{50} of 76 μM was calculated (Figure 3b). ATP activates the ryanodine receptor at 30-fold higher concentrations (EC_{50} 2.2 mM; see ref. [9]). This comparison confirmed that oATP displays a higher affinity for the nucleotide binding pocket than does ATP. The EC_{50} of 76 μM is lower than that determined in the $^{45}Ca^{2+}$ release measurements. We believe that this discrepancy arises from the non-equilibrium conditions which prevail over the time-scale of < 1 s. A Hill coefficient of 1.9 was derived from the concentration–response curve (Figure 3c). Since the single-channel recordings were carried out under equilibrium conditions, i.e. after a steady state had been achieved, this Hill coefficient is truly indicative of positive co-operativity.

Similar to the oATP-induced $^{45}Ca^{2+}$ release in HSR vesicles (Figure 1b), gating of the purified oATP-activated ryanodine receptor was inhibited by millimolar concentrations of Mg^{2+} (Figure 4a). In addition, we have also investigated the interaction of the plant alkaloid ryanodine with the oATP-preactivated channel. At low concentrations ryanodine has been shown to produce a characteristic long-lasting subconductance state of the ryanodine receptor [27,28]. Figure 4(b) demonstrates that the oATP-preactivated ryanodine receptor was switched into this subconductance state following the addition of 10 μM ryanodine. Further addition of ryanodine up to 100 μM transferred the channel into a permanently blocked state. The results demonstrate that the basic pharmacology of the ryanodine receptor/Ca^{2+}-release channel is preserved in the presence of oATP.

Covalent labelling of the ryanodine receptor adenine nucleotide binding site

The fact that oATP not only induced Ca^{2+} release from the SR but also activated the purified ryanodine receptor in single-channel recordings suggested that it acts via a direct interaction with an adenine nucleotide binding site of the channel protein. However, the possibility cannot be ruled out that the effect of oATP is mediated via additional, as yet unidentified, components which may be associated with the ryanodine receptor in the SR.

We therefore synthesized [α-^{32}P]oATP to directly identify and label the adenine nucleotide binding site of the purified ryanodine receptor. The experimental strategy relies on the assumption that the two aldehyde groups in positions 2′ and 3′ of oATP form a Schiff base with the ϵ-amino group of a lysine residue within the adenine nucleotide binding pocket. The Schiff base was converted to a stable covalent bond by borhydride reduction in order to visualize the incorporation (Figure 5). At the concentration employed the stoichiometry of the final incorporation was in the range 1–10%, as determined by counting the radioactivity in the gel slices of the [α-^{32}P]oATP-labelled ryanodine receptor (results not shown). This value does not account for losses of the protein during sample preparation. The incorporation of [α-^{32}P]oATP into the ryanodine receptor was decreased by concomitant addition of a 20-fold molar excess of ADP (Figure 5a, lane 5). Similarly, increasing concentrations of ATP and oATP competed with [α-^{32}P]oATP (Figure 5b); oATP was more potent than the parent nucleotide ATP. This is consistent with the higher affinity of oATP than of ATP determined in the single-channel recordings. A modest degree of incorporation was also seen into the 170 kDa protein (Figure 5a, lanes 1 and 4), which is probably a proteolytic fragment of the ryanodine receptor [29,30]. The labelling of this fragment was also inhibited by ADP (Figure 5a, lane 5) as well as by ATP and oATP (results not shown).

The binding of [α-^{32}P]oATP reached a maximum after 10–15 min and remained stable for up to 30 min (Figure 5c). If a 1000-fold molar excess of ATP was added after the equilibrium had been reached (i.e. after 15 min), the incorporation of [α-^{32}P]oATP was unaffected (Figure 5c, lane 5). In contrast, if a similar molar excess was added concomitantly, labelling was reduced by about 90% (Figure 5b, lane 4). This shows that oATP binds in a quasi-irreversible manner and that Schiff base formation prevents nucleotide exchange. Similar results were recently obtained with periodate-oxidized GTP and periodate-oxidized guanosine 5′-[γ-thio]triphosphate binding to the purified recombinant G protein α-subunit [31,32].

DISCUSSION

ATP is not only a phosphate donor for energy-consuming processes but also a ligand for extracellular and intracellular

receptors. ATP acts from the extracellular side on P_2-purinoceptors [33] and from the intracellular side on ion channels, such as ATP-ligand K^+ channels [34–36] and the ryanodine receptor [11–14]. In contrast to ATP-dependent K^+ channels, the physiological relevance of the adenine nucleotide-dependent modulation of the ryanodine receptor is poorly understood. The primary sequence of the ryanodine receptor does not unambiguously identify a typical nucleotide binding site. The consensus sequence GXGXXG [37] has been used to search for potential binding sites by groups who have deduced the amino acid sequence. Two candidate regions have been proposed: one is located within the N-terminal region and the second is on the N-terminal side of the predicted transmembrane-pore-forming α-helices [15,16]. Studies of the ryanodine receptor are complicated by the huge size of the molecule, which makes a structure–function analysis by mutagenesis currently impossible. In order to obtain structural and functional information about the adenine nucleotide binding site of the ryanodine receptor, we have thus employed the 2′,3′-dialdehyde analogue of ATP, oATP, as a ligand. Similar to ATP, the parent nucleotide, oATP stimulates $^{45}Ca^{2+}$ efflux from SR vesicles and activates the purified ryanodine receptor in artificial lipid bilayers. An explanation for the modest differences in EC_{50} values calculated from the concentration–response curves obtained with the two methods is given in the Results section. The apparent affinity of oATP surpasses that of ATP by a factor of 20–30. This is to be expected. The binding of oATP results in the formation of a Schiff base with lysine side-chains in the binding pocket. This quasi-irreversible binding decreases the off-rate and therefore increases the apparent affinity. Evidence for this interpretation is also provided by the observation that subsequent addition of a large molar excess of ATP fails to dissociate oATP prebound to the ryanodine receptor. Analogous results were recently obtained in experiments in which the binding of periodate-oxidized GTP (oGTP) to G protein α-subunits was studied [31,32].

The ability of the ryanodine receptor to respond to other regulatory ligands is not impaired by the quasi-irreversible binding of oATP. The oATP-stimulated channel activity is blocked by millimolar concentrations of Mg^{2+}, indicating that oATP neither inhibits access to the Mg^{2+} binding site nor interferes with the closing mechanism of the channel protein. Similarly, the concentration-dependent effects of ryanodine, i.e. induction of the typical subconductance state and blocking of ion flux through the channel, can be observed in the oATP-activated channel. Hence the basic regulation of the Ca^{2+}-release channel is retained in the presence of the ATP analogue. In line with these findings, oATP also stimulates [^{3}H]ryanodine binding at both low and high ryanodine concentrations (results not shown).

The concentration–response curves for oATP obtained with both the Ca^{2+} flux measurements and the single-channel recordings are steep. A Hill coefficient of approx. 2 was calculated for both data sets. As mentioned earlier, the data derived from the Ca^{2+} release experiments must be viewed with caution due to the non-equilibrium conditions that prevail over the very short time-scale. However, the Hill coefficient derived from the single-channel recordings does not suffer from this limitation. In addition, a comparable Hill coefficient has been determined for ATP-induced $^{45}Ca^{2+}$ release [12], and slopes of 3.3 and 2.1 have been reported for Ca^{2+} release induced with the adenosine 5′-oligophospho-5′-adenosines Ap_6A and Ap_5A respectively [38]. Hence the adenine nucleotide binding sites apparently function in a co-operative manner in the tetrameric protein, and this co-operativity is not impeded by oATP. Taken together, the results indicate that, in spite of the structural modification (namely the opening of the ribose ring), oATP is functionally equivalent to ATP.

The two aldehyde groups of oATP can form Schiff bases by interacting with the ϵ-amino group of lysine residues in the nucleotide binding cleft. This allows for the covalent incorporation of oATP into the ryanodine receptor after borhydride reduction. Direct labelling of a nucleotide binding site on the ryanodine receptor has also been demonstrated with the photoaffinity ligands 8-azido-[α-^{32}P]ATP [3] and 3′-*o*-(4-benzoyl)-[α-^{32}P]ATP [39]. However, to our knowledge, no functional data have been published for these analogues. The three analogues differ with respect to the modification introduced. 8-Azido-ATP will identify amino acid residues in the vicinity of the purine base. 3′-*o*-(4-Benzoyl)-ATP carries a bulky substituent that presumably labels a hydrophobic area within the nucleotide binding pocket. oATP specifically labels lysine residues within the ribose binding region. Hence the three compounds should yield complementary information about the structure of the nucleotide binding cleft on the ryanodine receptor.

In contrast to the ryanodine receptor, where adenine nucleotides stimulate channel gating, ATP induces channel closure in ATP-dependent K^+ channels [35,36]. However, a typical adenine nucleotide binding site has not been identified in the primary sequence of the ATP-dependent K^+ channel [34]. We believe that oATP may thus be a useful tool with which to study the structure and function not only of the ryanodine receptor but also of ATP-dependent K^+ channels as well as other ion channels which may be directly regulated by nucleotides.

We are grateful to Dr. M. Freissmuth for helpful discussions and critical reading of the manuscript, and to E. Tuisl and E. Weisz for artwork. M.H. was supported by a grant from the Fond zur Förderung der wissenschaftlichen Forschung (S-6044 to M. Freissmuth).

REFERENCES

1 Endo, M. (1977) Physiol. Rev. **57**, 71–108
2 Martonosi, A. N. (1984) Physiol. Rev. **64**, 1240–1320
3 Lai, F. A., Erikson, H. P., Rousseau, E., Liu, Q. Y. and Meissner, G. (1988) Nature (London) **331**, 315–319
4 Hymel, L., Inui, M., Fleischer, S. and Schindler, H. (1988) Proc. Natl. Acad. Sci. U.S.A. **85**, 441–445
5 Smith, J. S., Imagawa, T., Ma, J., Fill, M., Campbell, K. P. and Coronado, R. (1988) J. Gen. Physiol. **92**, 1–26
6 Palade, P., Dettbarn, C., Brunder, D., Stein, P. and Hals, G. (1989) J. Bioenerg. Biomembr. **21**, 295–320
7 Witcher, D. R., Kovacs, R. J., Schulmann, H., Cefali, D. C. and Jones, L. R. (1991) J. Biol. Chem. **266**, 11144–11152
8 Wang, J. and Best, P. M. (1992) Nature (London) **359**, 739–741
9 Herrmann-Frank, A. and Varsányi, M. (1993) FEBS Lett. **332**, 237–242
10 Hohenegger, M. and Suko, J. (1993) Biochem. J. **296**, 303–308
11 Meissner, G. (1984) J. Biol. Chem. **259**, 2365–2374
12 Meissner, G., Darling, E. and Eveleth, J. (1986) Biochemistry **25**, 236–244
13 Smith, J. S., Coronado, R. and Meissner, G. (1985) Nature (London) **316**, 446–449
14 Smith, J. S., Coronado, R. and Meissner, G. (1986) J. Gen. Physiol. **88**, 573–588
15 Takeshima, H., Nishimura, S., Matsumoto, T., Ishida, H., Kangawa, K., Minamino, N., Matsuo, H., Ueda, M., Hanaoka, M., Hirose, T. and Numa, S. (1989). Nature (London) **339**, 439–445.
16 Zorzato, F., Fuji, J., Otsu, K., Phillips, M., Green, M. N., Lai, A. F., Meissner, G. and MacLennan, D. H. (1990) J. Biol. Chem. **265**, 2244–2256
17 Hohenegger, M. and Makinose, M. (1992) Eur. J. Biochem. **205**, 173–179
18 Easterbook-Smith, S. B., Wallace, J. C. and Keech, D. B. (1976) Eur. J. Biochem. **62**, 125–130
19 Wyskovsky, W., Hohenegger, M., Plank, B., Hellmann, G., Klein, S. and Suko, J. (1990) Eur. J. Biochem. **194**, 549–559
20 Suko, J., Maurer-Foby, I., Plank, B., Bertl, O., Wyskovsky, W., Hohenegger, M. and Hellmann, G. (1993) Biochim. Biophys. Acta **117**, 193–206
21 Moutin, M. J. and Dupont, Y. (1988) J. Biol. Chem. **263**, 4228–4235
22 Laemmli, U. K. (1970) Nature (London) **227**, 680–685
23 Lowry, O. H., Rosebrough, N. J., Farr, A. L. and Randall, R. J. (1951) J. Biol. Chem. **193**, 265–275

24 Kaplan, R. S. and Pedersen, P. L. (1985) Anal. Biochem. **150**, 97–104
25 Fabiato, A. (1988) Methods Enzymol. **157**, 378–417
26 Morii, H. and Tonomura, Y. (1983) J. Biochem. (Tokyo) **94**, 1101–1109
27 Rousseau, E., Smith, J. S. and Meissner, G. (1987) Am. J. Physiol. **253**, C364–C368
28 Nagasaki, K. and Fleischer, S. (1988) Cell Calcium **9**, 1–7
29 Inui, M., Saito, A. and Fleischer, S. (1987) J. Biol. Chem. **262**, 15637–15642
30 Lai, A. F., Erikson, H., Block, B. and Meissner, G. (1987) Biochem. Biophys. Res. Commun. **143**, 704–709
31 Hohenegger, M., Nanoff, C., Ahorn, H. and Freissmuth, M. (1994) J. Biol. Chem. **269**, 32008–32015
32 Nanoff, C., Boehm, S., Hohenegger, M., Schütz, W. and Freissmuth, M. (1994) J. Biol. Chem. **269**, 31999–32007
33 Barnard, E. A., Burnstock, G. and Webb, T. E. (1994) Trends Pharmacol. Sci. **15**, 67–70
34 Ho, K., Nichols, G. C., Lederer, W. J., Lytton, J., Vassiev, P. M., Kanazirska, M. V. and Hebert, S. C. (1993) Nature (London) **362**, 31–38
35 Edwards, G. and Weston, A. (1993) Annu. Rev. Pharmacol. Toxicol. **33**, 597–637
36 Terzic, A., Tung, R. T. and Kurachi, Y. (1994) Cardiovasc. Res. **28**, 746–753
37 Wierenga, R. K. and Hol, W. G. J. (1983) Nature (London) **302**, 842–844
38 Morii, H. and Makinose, M. (1992) Eur. J. Biochem. **205**, 979–984
39 Zarka, A. and Shoshan-Barmatz, V. (1993) Eur. J. Biochem. **213**, 147–154

Received 30 August 1994/19 December 1994; accepted 12 January 1995